



**Adaptable Ligand Donor Strength: Tracking Transannular
Bond Interactions in Tris(2-pyridylmethyl)-
azaphosphatrane (TPAP)**

Journal:	<i>Dalton Transactions</i>
Manuscript ID	DT-ART-08-2018-003180.R1
Article Type:	Paper
Date Submitted by the Author:	12-Sep-2018
Complete List of Authors:	Thammavongsy, Zachary; University of California Irvine, Cunningham, Drew; University of California-Irvine, Chemistry Sutthirat, Natwara; University of California, Irvine, Chemistry Eisenhart, Reed; University of Minnesota, Minneapolis, Department of Chemistry Ziller, Joseph; University of California, Irvine, Department of Chemistry Yang, Jenny; University of California, Irvine, Chemistry

Adaptable Ligand Donor Strength: Tracking Transannular Bond Interactions in Tris(2-pyridylmethyl)-azaphosphatrane (TPAP)

Zachary Thammavongsy[†], Drew W. Cunningham[†], Natwara Sutthirat[†], Reed J. Eisenhart[‡], Joseph W. Ziller[†], Jenny Y. Yang^{†*}

[†]Department of Chemistry, University of California, Irvine, California 92697, United States

[‡]Department of Chemistry, University of Minnesota, Minneapolis, Minnesota 55455, United States

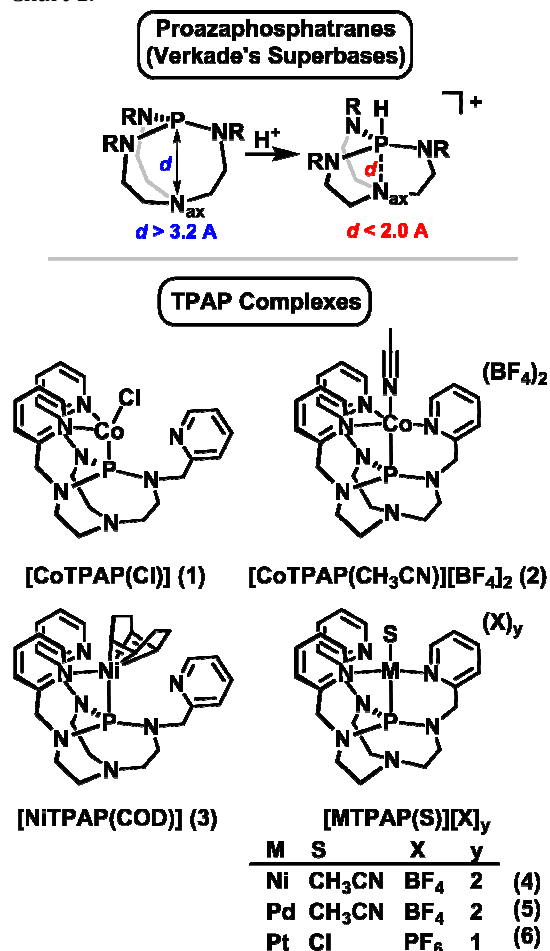
ABSTRACT: Flexible ligands that can adapt their donor strength have enabled unique reactivity in a wide range of inorganic complexes. Most examples are composed of flexible multi-dentate ligands containing a donor that can vary its interaction through its distance to the metal center. We describe an alternative type of adaptable ligand interaction in the neutral multi-dentate ligand tris(2-pyridylmethyl)-azaphosphatrane (TPAP), which contains a proazaphosphatrane unit. Proazaphosphatranes are intrinsically strong phosphorous donors; upon coordinated to more Lewis acidic atoms the phosphorous can accept additional electron density from a tertiary nitrogen to form a transannular bond, increasing its donor strength. An experimental and computational investigation of the varying degree of transannular interaction in TPAP when coordinated to late transition metals is reported. The synthesis and characterization of the complexes M(TPAP), where M = Co(I)Cl, Ni(0)(1,5-cyclooctadiene), Ni(II)(CH₃CN)(BF₄)₂, Pd(II)(CH₃CN)(BF₄)₂, Pt(II)Cl(PF₆) is described. Structural characterization and density functional theory calculation of these complexes, along with the previously reported [Co(II)(TPAP)(CH₃CN)](BF₄)₂ establish significant increases in the degree of transannular interaction of the proazaphosphatrane unit when coordinated to more electron deficient metal ions.

Introduction

Ligands that can adapt their donor strength provide a versatile method for adjusting electronic structure in order to access reactive transition metal intermediates. For example, Peters et al. have extensively explored first row metal complexes with tripodal phosphine ligands containing a B, C, or Si heteroatom, where the interaction between the metal and heteroatom adjusts depending on the metal oxidation state and identity of ligands trans to the interaction.¹ Parkin et al. have demonstrated that the flexible interactions of an apical carbon in atrane-type ligands contribute to unique reactivity,² and that the interaction can be modified through ligand design.³ Lu et al. designed tripodal ligands that encapsulate a Lewis acidic cation that can tune the electronic structure and reactivity at the metal.⁴ In addition, the Agapie⁵ and Meyer⁶ labs have utilized phenyl or mesitylene linkers strategically positioned near a metal to serve as electron reservoirs to support multi-electron reactivity. In all of the above cases, the adaptable interaction is incorporated into flexible chelating ligands, and the degree of interaction can be evaluated by the metal-donor distance. Under some conditions the weak interaction is absent, formally changing the coordination environment around the metal and thus the electronic structure.

In this study, we describe in detail an alternative type of adaptable interaction. The metal and donor maintain a fixed distance, but the latter can harness electron density through a transannular interaction when coordinated to more electron deficient metals. The ligand is based on proazaphosphatranes, a structurally unique class of neutral organic superbases more commonly known as Verkade's Superbases (Chart 1, top).⁷ These superbases are often used as a stoichiometric or catalytic Lewis base in a variety of organic transformations.⁸ The pK_a of the protonated form, or azaphosphatrane, ranges from 32.8 to 34.5 in acetonitrile depending on the substituents attached to the equatorial nitrogens (R).⁹ The extreme basicity of

Chart 1.



proazaphosphatranes stems from the formation of a stable three-centered four-electron transannular bond¹⁰ between P and N_{ax} upon protonation, shown as a dashed line on the top of Chart 1.^{7d, 8b, 11}

Verkade et al. previously utilized the P---N_{ax} distance as a useful indicator for evaluating the extent of the transannular interaction. Proazaphosphatranes have P---N_{ax} distances measured by X-ray crystallography of > 3.2 Å (3.35 Å is the sum of the van der Waals radii, which assumes no bonding interactions between P and N_{ax}).^{7e, 12} In contrast, azaphosphatranes have P---N_{ax} distances of under 2.0 Å (compared to the two-electron covalent radius between P and N_{ax} of 1.72 Å), providing structural evidence for the transannular interaction.

In addition to protons, Verkade et al. also explored the interaction of azaphosphatranes with Lewis acidic main group acceptors. In these derivatives, the P---N_{ax} distance varies between 2.55 (X = NHPH) and 3.28 (X = CH₂) Å (black circles, Figure 1). These intermediate, or “quasi” structures represent distances between the sum of the van der Waals of P and N (3.35 Å) and covalent transannular bond distance in protonated Verkade’s Superbase (R = Me, 1.97 Å).^{7c} Verkade noted a correlation with the degree of transannular interaction and the Lewis acidity of the substituent on P, with the strongest interaction with a proton.¹³

Although azaphosphatranes have been used as ligands in palladium-catalyzed C-C,¹⁴ C-N,¹⁵ cross-coupling and platinum-catalyzed hydrosilylation,¹⁶ the transannular interaction upon coordination to transition metal complexes had not been systematically interrogated.^{12a, 13, 17} The dynamic nature of azaphosphatranes led us to investigate whether the P---N_{ax} distance would adjust to different metals and oxidation states according to their Lewis acidity.

To provide greater coordinative stability, a proazaphosphatrane unit was incorporated in a tetradentate ligand to form (tris(2-pyridylmethyl)-azaphosphatrane, TPAP, shown in Chart 1.^{17a, 17b} The proazaphosphatrane in TPAP retains its ability to form a transannular bond; structural characterization of the protonated TPAP has a P---N_{ax} distance of 1.97(16) Å.^{17b} All three pyridine arms in TPAP can potentially coordinate to the metal ion, as illustrated in our previously published [Co(II)(CH₃CN)TPAP][BF₄]₂ complex (**2**),^{17b} but for some of the complexes reported herein only one or two pyridine arms are coordinated.

In this study, we discuss the structural and computational investigation of TPAP coordinated to two different metals in two different oxidation states: Co(I), Co(II) and Ni(0), Ni(II), as well as the TPAP complexes of Pd(II) and Pt(II), shown in Chart 1 as complexes **1-6**. The P---N_{ax} transannular distance was determined through structural characterization by X-ray crystallography. The varying degree of transannular interactions evident in the solid-state is supported by computational studies on the orbital interactions between the P and N_{ax} atoms in complexes **1, 2, 4, 5**, and **6** and an analogue of complex **3**.

Results

Synthesis and structure of CoTPAP complexes. The ligand TPAP was synthesized as previously reported.^{17b} The purple complex [CoTPAP(Cl)] (**1**) was prepared by adding stoichiometric amounts of TPAP to Co(I)Cl(PPh₃)₃ in tetrahydrofuran. Complex **1** is paramagnetic with a solution μ_{eff} of 3.34 μ_{B} (C₆D₆), corresponding to an S = 1

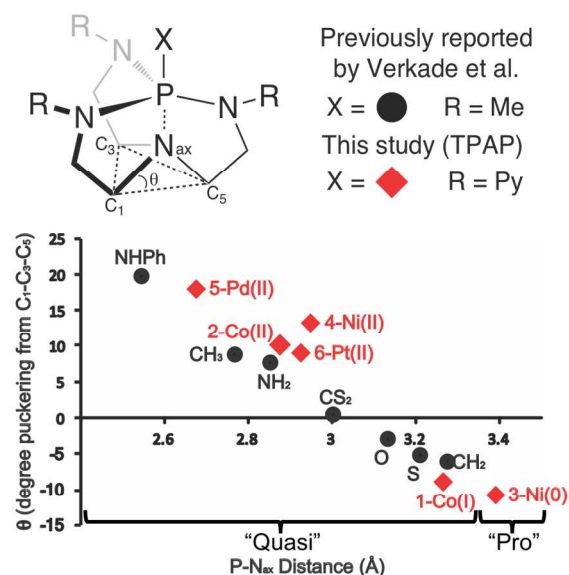


Figure 1. (top) Depiction of the angle, θ , as the degree of puckering of the apical nitrogen (red) out of the C-C-C plane. (bottom) Plot of the transannular distance versus the θ puckering of the axial nitrogen above the plane of the three adjacent carbon atoms for Verkade’s Superbase with various main groups (denoted in black circles ●) and TPAP with various transition metals (denoted in red diamonds ◆). Values used in this figure are from structural data.

system. Elemental analysis was used to confirm the analytical purity of the complex. X-ray quality crystals were grown from diethyl ether at -35 °C. The solid-state structure of complex **1** is shown in Figure 2 and selected bond distances and angles are shown in Table 1. The pseudo-tetrahedral cobalt center has a τ_4 parameter of 0.77, where a value of 1 represents an ideal tetrahedral geometry, and a value of 0 represents an ideal square planar geometry.¹⁸ The TPAP ligand chelates in a tridentate fashion through the phosphorus donor and two of the three pyridine N atoms. The fourth coordination site is occupied by a chloride ion. In **1**, TPAP has a transannular P---N₁ distance of 3.2647(14) Å and θ (puckering of the axial nitrogen above the plane of the three adjacent carbon atoms) of -9.1349° (Figure 2, Table 1).

The synthesis and structural characterization of divalent [CoTPAP(CH₃CN)][BF₄]₂ (**2**) was previously reported; selected bond distances and angles of **2** are shown in Table 1.^{17b}

Synthesis and structure of Group 10 TPAP complexes. [NiTPAP(COD)] (**3**) was synthesized through the reaction of stoichiometric amounts of TPAP with Ni(COD)₂ in tetrahydrofuran; the crude product was recrystallized from diethyl ether. Complex **3** is diamagnetic and was characterized by ¹H and ³¹P NMR spectroscopy (Figure S1 & S2). X-ray quality crystals of **3** were grown from a concentrated solution in diethyl ether at -35 °C; the solid-state structure is shown in Figure 2. In **3**, TPAP coordinates in a bidentate fashion through the phosphorus donor and one of the pyridines. The P---N₁ distance is 3.3915(17) Å and θ is -10.9882° (Table 1).

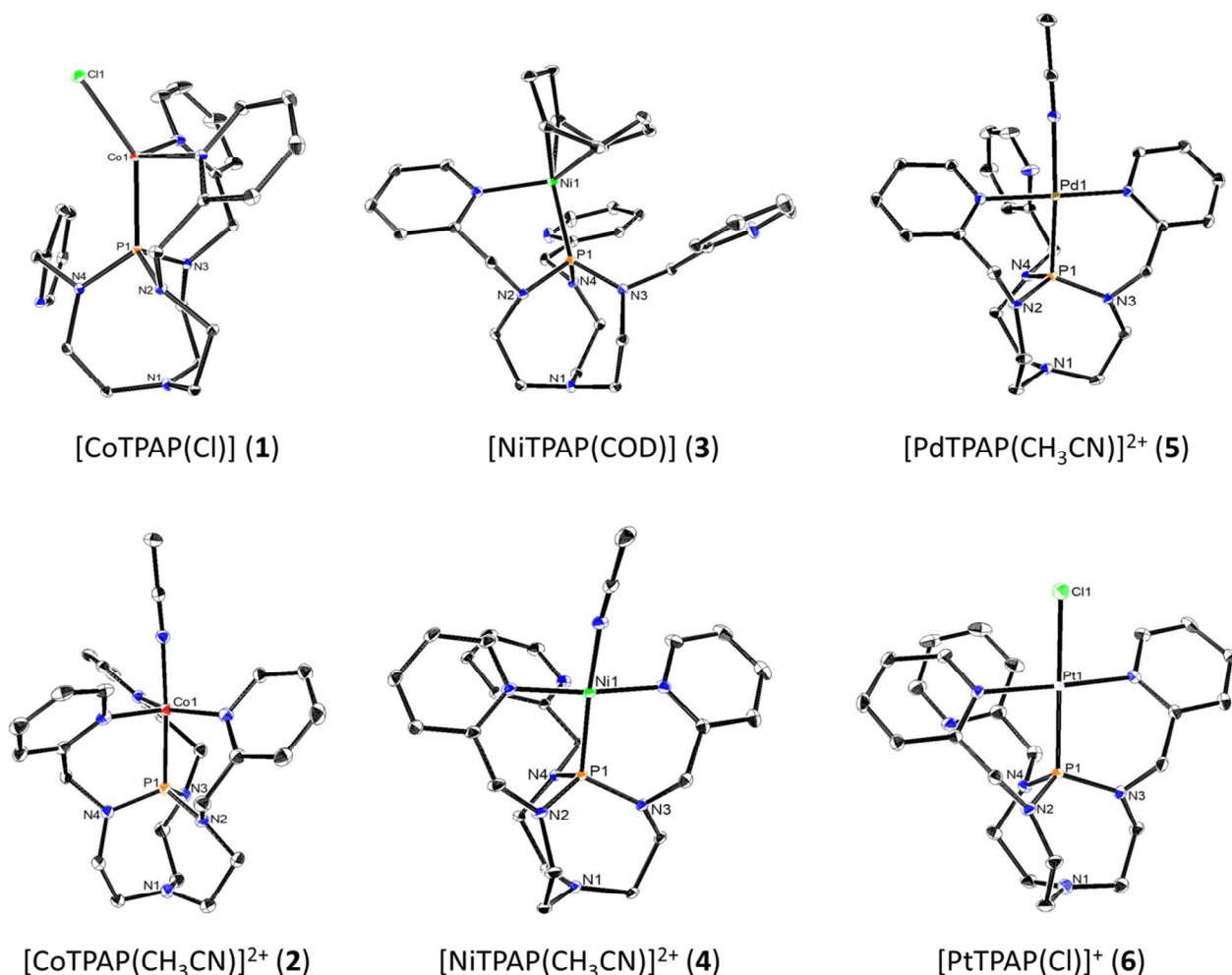


Figure 2. ORTEP of complexes **1**, **2**, **3**, **4**, **5** and **6**. Structures **5** and **6** display one of two molecules in the asymmetric unit. Thermal ellipsoids drawn at 50% probability. Hydrogen atoms and counteranions are omitted for clarity. Electron density from minor disorder of the Pt atom in **6** is also omitted.

Table 1. Bond lengths and angles of complexes **1-6**. Metrics **5** and **6** were taken from one of two molecules in the asymmetric unit. Metal ion is denoted as M. Non-italicized values are from the X-ray structural analysis and italicized values are from the geometry optimized structures calculated using quantum mechanical methods.

	1	2	3	4	5	6
P₁-N₁ (P---N_{ax}) (Å)	3.2647(14)	2.877(2)	3.3915(17)	2.948(2)	2.6747(18)	2.927(4)
<i>Calc. (P---N_{ax}) (Å)</i>	<i>3.088</i>	<i>2.737</i>	<i>3.306</i>	<i>2.701</i>	<i>2.646</i>	<i>2.815</i>
P₁-N₂ (Å)	1.7089(13)	2.035(2)	1.7101(16)	1.6500(19)	1.6722(17)	1.666(4)
P₁-N₃ (Å)	1.6892(13)	1.997(2)	1.6965(16)	1.6511(19)	1.6528(17)	1.649(4)
P₁-N₄ (Å)	1.6879(13)	2.094(2)	1.7007(16)	1.649(2)	1.6583(16)	1.642(4)
P₁-M (Å)	2.1675(5)	2.1693(7)	2.1642(5)	2.1670(7)	2.2294(5)	2.2245(11)
<i>Calc. P-M (Å)</i>	<i>2.190</i>	<i>2.263</i>	<i>2.323</i>	<i>2.254</i>	<i>2.357</i>	<i>2.354</i>
C₁-C₃-C₅ θ (°)	-9.1349	9.9140	-10.9882	13.0123	17.7932	8.8644
<i>Calc. C₁-C₃-C₅ θ (°)</i>	<i>3.41</i>	<i>16.62</i>	----	<i>17.32</i>	<i>18.62</i>	<i>13.79</i>

The divalent complexes [NiTPAP(CH₃CN)][BF₄]₂ (**4**) and [PdTPAP(CH₃CN)][BF₄]₂ (**5**) were synthesized by reaction of TPAP to the respective metal precursors in acetonitrile and recrystallized by layering with diethyl ether. Complexes **4** and **5** are diamagnetic and were characterized by ¹H and ³¹P NMR spectroscopy (Figure S3-

S5). X-ray quality crystals were obtained using the same method. The solid-state structures of **4** and **5** are shown in Figure 2 and selected bond distances and angles are shown in Table 1. Both **4** and **5** are four coordinate square planar complexes with τ₄ values of 0.20 and 0.06, respectively.

Table 2. Results of NBO Analysis of Donor-Acceptor Interactions in Compound Adducts, Estimated by Second-Order Perturbation Theory, $E^{(2)}_{i,j}$ (kcal/mol).

Parameter	1	2	3b	4	5	6
$LP(N_{ax}) \rightarrow \sigma^*(M-P)$	<0.5	1.09	<0.5	2.09	7.23	3.11
$LP(N_{ax}) \rightarrow \sigma^*(P-N)^a$	<1.5	2.86	<1.5	6.74	8.05	4.22

^a: These values are the sum of the three $LP(N_{ap}) \rightarrow \sigma^*(P-N)$.

The $P \cdots N_1$ distances of **4** and **5** are 2.948(2) and 2.6747(18) Å ($P_2 \cdots N_9 = 2.6613(18)$ Å), respectively.

[PtTPAP(Cl)][PF₆] (**6**) was synthesized in two steps. PtCl₂(COD) was first added to TPAP in acetonitrile. After one hour, two equivalents of AgPF₆ were added in the dark and the solution was stirred for 5 minutes. A colorless crystal was grown from diethyl ether and acetonitrile. Complex **6** is diamagnetic and was characterized by ¹H and ³¹P NMR spectroscopy (Figure S6 & S7). The solid-state structure of **6** is shown in Figure 2 and selected bond distances and angles are shown in Table 1. The coordination environment of **6** is similar to that of **4** and **5**, except an acetonitrile ligand is replaced by a chloride anion in the inner sphere. Complex **6** is closer to a square planar coordination geometry, with a τ_4 values of 0.12. TPAP in **6** displayed a $P \cdots N_1$ distances of 2.927(4) Å ($P_2 \cdots N_8 = 2.821(4)$ Å), with θ of 8.8644°.

Quantum Mechanical Calculations. DFT calculations were performed using the Gaussian program suite with the incorporate NBO 3.1 package¹⁹ at the M06²⁰ level of theory with 6-311G++(3df,3pd) basis set for 3rd row main groups, 6-311G**++ basis set for 2nd row main groups, and LANL2DZ basis set for all metals. Geometry optimizations of the complexes from the X-ray coordinates, followed by harmonic frequency calculations indicated that all of the compounds are minima on the potential energy surface. A comparison of selected calculated and experimental geometrical parameters is tabulated in Table 1.

Discussion

CoTPAP complexes. The $P \cdots N_1$ (or $P \cdots N_{ax}$) distance of TPAP when bound to a Co(I) ion in complex **1** (3.2647(14) Å) indicates a minimal transannular interaction with a value closer to the “pro” (or free base) rather than the “quasi” form. An additional crystal of **1**, complex **1b** was grown by pentane diffusion into a concentrated tetrahydrofuran solution (Figure S8) and exhibited a $P \cdots N_1$ distance in TPAP of 3.339(2) Å, a difference of 0.0743 Å between structures. Verkade observed that differences in crystal packing could influence the transannular distance by up to 0.1 Å, providing an estimated boundary for error in the solid-state distances.^{7f} The transannular distance observed in both Co(I) structures is comparable to those found when proazaphosphatranes is coordinated to main group elements such as sulfur and oxygen (Figure 1).²¹

Upon coordination of TPAP to a more Lewis acidic Co(II) ion (complex **2**), the $P \cdots N_1$ distance shortens to 2.877(2) Å, a significant shift of 0.39 Å. In Figure 1,

complex **2** is in the middle of the plot (“quasi” form of azaphosphatranes).

Group 10 complexes. Complex **3**, with a Ni(0) ion, has a $P \cdots N_1$ distance of 3.3915(17) Å, outside of the van der Waals radii of $P \cdots N$ and signifying no transannular interaction. The $P \cdots N_1$ distance of **3** falls within the range of four other previously reported Ni(0)azaphosphatranes complexes that bind in a monodentate fashion.^{17a} The consistent $P \cdots N_{ax}$ across the series highlights the fact that denticity of TPAP has little influence on the $P \cdots N_{ax}$ transannular interaction compared to monodentate azaphosphatranes when Ni(0) is bound. When TPAP is bound to a Ni(II) ion in complex **4**, the $P \cdots N_1$ distance shortens to 2.948(2) Å, which lies within the “quasi” form of azaphosphatranes. As seen in the CoTPAP case, there is a significant decrease in the $P \cdots N_1$ transannular distance with an increase in oxidation state of the Ni metal center.

The Pd(II) and Pt(II) TPAP complexes (**5** and **6**) were also investigated in order to determine if the transannular distance changes upon coordination to larger metal ions. The transannular distance decreases by 0.273 Å from Ni(II) to Pd(II), whereas the $P \cdots N_1$ distance in Pt(II) resembles that of Ni(II). The chloride ligand in **6** could increase the $P \cdots N_1$ distance due to the π donation of Cl⁻, which would decrease the Lewis acidity of the Pt metal center.^{7c, 22} We were unable to experimentally isolate a Pt(II) complex with an acetonitrile ligand by adding AgBF₄ to **6**; as a result, we cannot quantify the effect of the Cl⁻ anion on the Pt(II) center. A computational analysis of a Pd(II) analogue with a Cl⁻ anion and a Pt(II) analogue with an acetonitrile ligand indicate the $P \cdots N_{ax}$ distance is close for Pd(II) and Pt(II) when they have the same fourth ligand. (see Table S39 and accompanying details). However, the $P \cdots N_{ax}$ distance is consistently larger when Pd(II) or Pt(II) is bound by a Cl⁻ anion compared to CH₃CN.

Oxidation State Effects. Verkade found that the $P \cdots N_{ax}$ distance in azaphosphatranes is influenced by the Lewis acidity of the atom or group when bound to the phosphorus. When coordinated to Ni and Co, the $P \cdots N_{ax}$ distance decreases with increasing oxidation state of the metal (and concomitant increase in Lewis acidity of the metal ion). As the oxidation state increases from Co(I) to Co(II), θ increases by 19.05° and the $P \cdots N_1$ distance contracts by 0.39 Å (Table 1, Co(I) and Co(II)). A more prominent trend is observed with Ni(0) and Ni(II), where θ increases by 24° and the $P \cdots N_1$ distance shortens by 0.44 Å upon oxidation (Table 1, Ni(0) and Ni(II)).

Computation. We propose the shortening of the $P \cdots N_{ax}$ distance with concomitant puckering of the axial nitrogen above the plane of the three adjacent carbon atoms (θ in Figure 1) is due to electron donation between the axial nitrogen (N_{ax}) and the phosphorus atom of the azaphosphatranes unit. To probe the nature of the $P \cdots N_{ax}$ interaction and observe electron density in a chemically intuitive manner, an analysis utilizing natural bond orbital (NBO) perturbation theory was carried out with a focus on the NBOs of the $M-P-N_{ax}$ fragment. All calculated values for each metal ion coordinated to TPAP utilized the complexes in Chart 1 except [NiTPAP(COD)] (**3**). The latter could not be modeled computationally because the structure failed to converge to a minimum on the potential energy surface. The previously reported structure [Ni(κ^1 -TPAP)(CO)]₂

(3b)^{17a} was used as an alternative model for the transannular interaction of a Ni(0) bound to TPAP. Table 2 summarizes the calculated stabilization energies for each compound.

When the oxidation state of the metal is greater than +1, there is significant donation from the lone pair (LP) of N_{ax} into unfilled antibonding NBOs. The LP(N_{ax})→σ*(M–P) stabilization is ca. 2 kcal/mol for the case of Ni(II) and Co(II). For Co(I) and Ni(0), where minimal or no transannular interaction is observed experimentally, the stabilization energy is negligible (<0.5 kcal/mol). For second- and third-row metals the LP(N_{ax})→σ*(M–P) interaction provides 7.2 kcal/mol and 3.1 kcal/mol of stabilization energy for Pd(II) and Pt(II), respectively. In addition to the LP(N_{ax})→σ*(M–P) donation, there is a significant interaction of the axial nitrogen with the three σ*(P–N) NBOs. (Table 2). These calculations suggest the interaction of the axial nitrogen with the phosphorus atom is the dominating factor that influences the puckering angle, θ, and P---N_{ax} distance.

The proposed interaction between the phosphorus atom and axial nitrogen can be seen by visualizing the highest occupied molecular orbitals (HOMO) for Ni(0) and Ni(II) (Figure 3). In the case of Ni(0), which lacks any significant P---N_{ax} interactions, the axial nitrogen contributes only 7% to the HOMO and does not interact with any orbitals of phosphorus; however, for Ni(II) the axial nitrogen contributes 51% to the HOMO and results in a shortening on the P---N_{ax} as well as a positive value of θ.

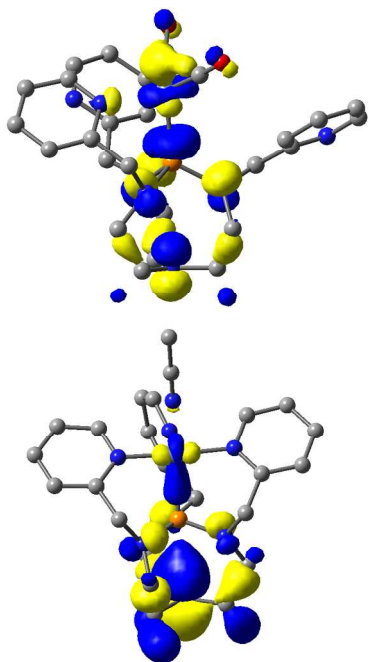


Figure 3. HOMOs of Ni(0) (Top) and Ni(II) (Bottom). All surfaces are at an isovalue of 0.035.

Conclusion

The use of flexible ligands with adjustable coordinative interactions has shown great utility in accessing reactive metal sites. In this study, we demonstrate that an azaphosphatrane incorporated into a chelating ligand provides a new type of variable ligand interaction. The metal-ligand distance remains constant while the non-coordinating nitrogen in the

azaphosphatrane can donate additional electron density into the phosphorous ligand. We have previously measured the Tolman parameter of azaphosphatranes and found that even in the absence of a transannular interaction, they are among the most strongly donating phosphine ligands.^{17a} Thus, the TPAP ligand represents an inherently strong ligand that can increase its donor strength in contrast to prior systems that utilize weaker interactions. The higher donor strength available with TPAP may also be valuable for stabilizing more electron deficient metal ions.

Experimental Details

General Considerations. The complexes described below are air- and moisture-sensitive and must be handled under an inert atmosphere of nitrogen using standard glovebox and Schlenk techniques. Unless otherwise noted, all procedures were performed at ambient temperature (21–24 °C). All solvents were sparged with argon and dried using a solvent purification system. Acetonitrile, diethyl ether, and halogenated solvents were passed through two columns of neutral alumina. Compounds tris(2-pyridylmethyl)proazaphosphatrane^{17b}, CoCl(PPh₃)₃²³, and [Ni(CH₃CN)_{6.5}][BF₄]₂²⁴ were synthesized according to established procedures. CD₃CN and C₆D₆ were freeze-pump-thawed three times and dried over molecular sieves. [Pd(CH₃CN)₄][BF₄]₂, PtCl₂(COD) and AgPF₆ were purchased from commercial sources and used without further purification.

Physical Methods. Electrospray ionization mass spectrometry (ESI-MS) was performed with an ESI LC-TOF Micromass LCT 3 mass spectrometer in the Department of Chemistry at UC Irvine. Nuclear magnetic resonance (NMR) spectra were recorded on a DRX400 with a switchable QNP probe (¹H and ³¹P) or a Bruker AVANCE 600 MHz (¹H and ³¹P). All chemical shifts (δ) are reported in parts per million (ppm) relative to tetramethylsilane, and referenced to the residual protiated solvent peak. ³¹P^{12f} NMR spectroscopy experiments are referenced to the absolute frequency of 0 ppm in the ¹H dimension according to the Xi scale.²⁵ Elemental analyses were performed on a PerkinElmer 2400 Series II CHNS elemental analyzer.

X-ray Crystallography. X-ray diffraction studies were carried out at the UCI Department of Chemistry X-ray Crystallography Facility on a Bruker SMART APEX II diffractometer. Data were collected at 133 K for 1, 3, 5 and 6, and 88 K for 4 using Mo Kα radiation (λ = 0.710 73 Å). The APEX2 program package was used to determine the unit cell parameters and for data collection (60, 60, 35, 30 and 20 sec/frame scan time for a sphere of diffraction data for 1, 3, 4, 5 and 6, respectively). The raw frame data was processed using SAINT and SADABS to yield the reflection data file. Subsequent calculations were carried out using the SHELXTL program.

For structure 4, atoms F(7) and F(8) were disordered and included using multiple components with partial site-occupancy-factors.

For structure 5, atoms C(54), F(5), F(6), F(7) and F(8) were disordered and included using multiple components with partial site-occupancy-factors.

For structure 6, there were several high residuals present in the final difference-Fourier map. It was not possible to determine the nature of the residuals although it was probable that diethyl ether solvent was present. The SQUEEZE routine in the PLATON program package was used to account for the electrons in the solvent accessible voids.

Structural analysis for complex **1b** was carried out at the University of Minnesota, Minneapolis X-ray Crystallography Facility on a Bruker D8 Photon 100 CMOS diffractometer. Data was collected at 123 K.

[CoTPAP(CI)] (1). In the glove box, a solution of TPAP (34.2 mg, 0.076 mmol) in 5 mL tetrahydrofuran was added to a solution of CoCl(PPh₃)₃ (67.3 mg, 0.076 mmol) in 2 mL tetrahydrofuran. The solution immediately turned dark purple and was stirred for 1 day at room temperature. The solvent was removed under vacuum. The resulting purple solid was re-dissolved in diethyl ether and filtered through a glass pipette packed with a glass microfiber filter (22 μm). X-ray quality crystals were grown from a concentration solution of **1** in diethyl ether at -35 °C (28.7 mg, 0.053 mmol, 69.4% Yield). Analytical Calculation for C₂₄H₃₀ClCoN₇P: C, 53.19; H, 5.58; N, 18.09 Found: C, 53.67; H, 5.25; N, 17.45. μ_{eff} (solution) = 3.34 μ_B. ESI-MS data could not be obtained due to the air sensitivity of complex **1** in solution.

[NiTPAP(COD)] (3). In the glove box, a solution of TPAP (100 mg, 0.223 mmol) in 3 mL tetrahydrofuran was added to a solution of Ni(COD)₂ (61.5 mg, 0.223 mmol) in 7 mL tetrahydrofuran. The solution immediately turned dark green and was stirred for 1 day at room temperature. The solvent was removed under vacuum. The resulting green solid was re-dissolved in diethyl ether and filtered through a glass pipette packed with a glass microfiber filter (22 μm). X-ray quality crystals were grown from a concentration solution of **3** in diethyl ether at -35 °C. ¹H NMR (C₆D₆, 600 MHz) δ = 2.07 (s, 8H, COD), 2.64-2.84 (br, 12H, NCH₂CH₂N), 4.30 (s, 6H, PyCH₂), 4.43 (br, 4H, COD), 6.59 (t, 3H, Py), 7.08 (m, 3H, Py), 7.12 (t, 3H, Py), 8.68 (m, 3H, Py). ³¹P{¹H}NMR (C₆D₆, 243 MHz) δ = 150.7. Analytical Calculation for C₂₄H₃₀N₇NiP•(C₈H₁₂)_{0.5}: C, 64.68; H, 7.24; N, 14.67 Found: C, 64.04; H, 6.77; N, 14.29. ESI-MS data could not be obtained due to the air sensitivity of complex **3** in solution. The yield is not reported due to the presence of COD impurities in both the ¹H NMR and elemental analysis data.

[NiTPAP(CH₃CN)][BF₄]₂ (4). In the glove box, a solution of TPAP (109 mg, 0.250 mmol) in 7 mL of acetonitrile was added to a solution of [Ni(CH₃CN)_{6.5}][BF₄]₂ (122 mg, 0.250 mmol) in 2 mL of acetonitrile. The solution immediately turned dark orange and was stirred for 1 day at room temperature. The solvent was removed under vacuum. The resulting orange solid was re-dissolved in dichloromethane, filtered through a glass pipette packed with a glass microfiber filter (22 μm). X-ray quality crystals of **4** were grown from acetonitrile and diethyl ether (97.5 mg, 0.135 mmol, 55.1% Yield). ¹H NMR (CD₃CN, 400 MHz) δ = 2.82 (t, 6H, NCH₂CH₂N), 2.94 (t, 6H, NCH₂CH₂N), 4.50 (s, 6H, PyCH₂), 7.61 (m, 6H, Py), 7.97 (t, 3H, Py), 9.51 (s, 3H, Py). ESI-MS (m/z): [M - 2BF₄ - CH₃CN + Cl]⁺. Calculation for C₂₄H₃₀N₇PNiCl, 540.13; Found, 540.20. Analytical Calculation for C₂₆H₃₃B₂F₈N₈NiP: C, 43.32; H, 4.61; N, 15.54 Found: C, 43.65; H, 5.02; N, 15.18. Although the sample is analytically pure and the ¹H NMR is consistent with the proposed structure, we were unable to resolve a ³¹P{¹H} NMR resonance. The lack of a resonance may be due to fluxional coordination in solution.

[PdTPAP(CH₃CN)][BF₄]₂ (5). In the glove box, a solution of TPAP (81.0 mg, 0.181 mmol) in 6 mL of acetonitrile was added to a solution of [Pd(CH₃CN)₄][BF₄]₂ (80.1 mg, 0.181 mmol) in 2 mL of acetonitrile. The solution immediately turned orange and was stirred for 1 day at room temperature. The solvent was removed under vacuum. The resulting yellow solid was re-dissolved in acetonitrile, filtered through a glass pipette packed with a glass microfiber filter (22 μm). X-ray quality crystals of **5** were grown from acetonitrile and diethyl

ether (121 mg, 157 mmol, 86.9% Yield). ¹H NMR (CD₃CN, 400 MHz) δ = 2.72 (t, 6H, NCH₂CH₂N), 2.94 (m, 6H, NCH₂CH₂N), 4.45 (d, 6H, PyCH₂), 7.46 (m, 6H, Py), 7.97 (dt, 3H, Py), 8.66 (d, 3H, Py). ³¹P{¹H}NMR (CD₃CN, 162 MHz) δ = 50.8. ESI-MS (m/z): [M - 2BF₄ - CH₃CN + Cl]⁺ Calculation for C₂₄H₃₀N₇PPdCl, 588.1; Found, 588.0. Analytical Calculation for C₂₆H₃₃B₂F₈N₈PdP: C, 40.63; H, 4.33; N, 14.58 Found: C, 40.35; H, 4.20; N, 14.37.

[PtTPAP(CI)][PF₆]₂ (6). In the glove box, to a solution of TPAP (78.1 mg, 0.175 mmol) in 6 mL of acetonitrile was added to a solution of PtCl₂(COD) (65.3 mg, 0.175 mmol) in 6 mL acetonitrile. The solution immediately turned tan and was stirred for 1 h at room temperature. Then a solution of silver hexafluorophosphate (68.0 mg, 0.350 mmol) in 2 mL acetonitrile was added in the dark and stirred for 5 min. The solvent was removed under vacuum. The white solid was re-dissolved in dichloromethane and filtered through a medium fritted funnel. The solvent was removed under vacuum. The resulting white solid was re-dissolved in acetonitrile and filtered through a glass pipette packed with a glass microfiber filter (22 μm). The filtrate was recrystallized by addition of diethyl ether. Only single crystals of **6** were collected which contributed to the low yield of the pure sample. We did not make any further purification attempts on the crude product in order to increase the yield. X-ray quality crystals of **6** were grown from the same conditions as the recrystallization. (17.3 mg, 0.021 mmol, 12.1% Yield). ¹H NMR (CD₃CN, 600 MHz) δ = 2.64 (t, 2H, NCH₂CH₂N), 2.78 (m, 2H, NCH₂CH₂N), 2.89 (m, 6H, NCH₂CH₂N), 3.17 (m, 2H, NCH₂CH₂N), 3.97 (d, 2H, PyCH₂), 4.25 (dd, 2H, PyCH₂), 4.88 (dd, 2H, PyCH₂), 6.74 (d, 1H, Py), 7.27 (m, 1H, Py), 7.45 (t, 2H, Py), 7.61 (m, 3H, Py), 8.08 (t, 2H, Py), 8.41 (m, 1H, Py), 8.95 (m, 2H, Py). ³¹P{¹H}NMR (CD₃CN, 243 MHz) δ = 39.8. ESI-MS (m/z): [M - BF₄]⁺ Calculation for C₂₄H₃₀N₇PPtCl, 677.2; Found, 677.1. Analytical Calculation for C₂₄H₃₀ClF₆N₇P₂Pt: C, 35.02; H, 3.67; N, 11.91 Found: C, 34.96; H, 3.51; N, 11.84.

ASSOCIATED CONTENT

Supporting Information. CIF files (CCDC deposition numbers) for **1** (1827010), **1b** (1841335), **3** (1827011), **4** (1827012), **5** (1827013) and **6** (1827014). ¹H and ³¹P{¹H} NMR data for **3**, **5** and **6**. ¹H NMR for **4**. Computational data.

AUTHOR INFORMATION

Corresponding Author

*j.yang@uci.edu

Author Contributions

The manuscript was written through contributions of all authors. All authors have given approval to the final version of the manuscript.

ACKNOWLEDGMENT

We would like to thank Professor Ged Parkin for helpful discussions. This material is based on work supported by the U. S. Department of Energy, Office of Science, Office of Basic Energy Sciences under Award Number DE-SC0012150.

REFERENCES

- (a) Moret, M.-E.; Zhang, L.; Peters, J. C., A Polar Copper-Boron One-Electron σ-Bond. *Journal of the American Chemical Society* **2013**, *135* (10), 3792-3795; (b) Anderson, J. S.; Rittle, J.; Peters, J. C., Catalytic conversion of nitrogen to ammonia by an iron model complex. *Nature* **2013**, *501*, 84; (c) Rittle, J.; Peters, J. C., Fe-N₂/CO complexes that model a possible role for the interstitial C atom of FeMo-cofactor (FeMoco). *Proceedings*

- of the National Academy of Sciences **2013**, *110* (40), 15898-15903; (d) Creutz, S. E.; Peters, J. C., Catalytic Reduction of N₂ to NH₃ by an Fe–N₂ Complex Featuring a C-Atom Anchor. *Journal of the American Chemical Society* **2014**, *136* (3), 1105-1115; (e) Moret, M.-E.; Peters, J. C., N₂ Functionalization at Iron Metallaboratranes. *Journal of the American Chemical Society* **2011**, *133* (45), 18118-18121; (f) Anderson, J. S.; Moret, M.-E.; Peters, J. C., Conversion of Fe–NH₂ to Fe–N₂ with release of NH₃. *Journal of the American Chemical Society* **2013**, *135* (2), 534-537; (g) Del Castillo, T. J.; Thompson, N. B.; Suess, D. L. M.; Ung, G.; Peters, J. C., Evaluating Molecular Cobalt Complexes for the Conversion of N₂ to NH₃. *Inorganic Chemistry* **2015**, *54* (19), 9256-9262.
2. (a) Rauch, M.; Parkin, G., Zinc and Magnesium Catalysts for the Hydrosilylation of Carbon Dioxide. *Journal of the American Chemical Society* **2017**, *139* (50), 18162-18165; (b) Rauch, M.; Ruccolo, S.; Parkin, G., Synthesis, Structure, and Reactivity of a Terminal Magnesium Hydride Compound with a Carbatrane Motif, [TismPriBenz]MgH: A Multifunctional Catalyst for Hydrosilylation and Hydroboration. *Journal of the American Chemical Society* **2017**, *139* (38), 13264-13267; (c) Chakrabarti, N.; Ruccolo, S.; Parkin, G., Cadmium Compounds with an [N3C] Atrane Motif: Evidence for the Generation of a Cadmium Hydride Species. *Inorganic Chemistry* **2016**, *55* (23), 12105-12109.
3. (a) Ruccolo, S.; Sattler, W.; Rong, Y.; Parkin, G., Modulation of Zn–C Bond Lengths Induced by Ligand Architecture in Zinc Carbatrane Compounds. *J. Am. Chem. Soc.* **2016**, *138* (44), 14542-14545; (b) Ruccolo, S.; Rauch, M.; Parkin, G., Tris[(1-isopropylbenzimidazol-2-yl)dimethylsilyl]methyl metal complexes, [TismPriBenz]M: a new class of metallacarbatranes, isomerization to a tris(N-heterocyclic carbene) derivative, and evidence for an inverted ligand field. *Chemical Science* **2017**, *8* (6), 4465-4474.
4. (a) Rudd, P. A.; Planas, N.; Bill, E.; Gagliardi, L.; Lu, C. C., Dinitrogen Activation at Iron and Cobalt Metallalumatranes. *European Journal of Inorganic Chemistry* **2013**, *2013* (22□23), 3898-3906; (b) Vollmer, M. V.; Xie, J.; Lu, C. C., Stable Dihydrogen Complexes of Cobalt(–I) Suggest an Inverse trans-Influence of Lewis Acidic Group 13 Metalloligands. *Journal of the American Chemical Society* **2017**, *139* (19), 6570-6573; (c) Cammarota, R. C.; Lu, C. C., Tuning Nickel with Lewis Acidic Group 13 Metalloligands for Catalytic Olefin Hydrogenation. *Journal of the American Chemical Society* **2015**, *137* (39), 12486-12489; (d) Cammarota, R. C.; Vollmer, M. V.; Xie, J.; Ye, J.; Linehan, J. C.; Burgess, S. A.; Appel, A. M.; Gagliardi, L.; Lu, C. C., A Bimetallic Nickel–Gallium Complex Catalyzes CO₂ Hydrogenation via the Intermediacy of an Anionic d₁₀ Nickel Hydride. *J. Am. Chem. Soc.* **2017**, *139* (40), 14244-14250.
5. (a) Buss, J. A.; Agapie, T., Four-electron deoxygenative reductive coupling of carbon monoxide at a single metal site. *Nature* **2015**, *529*, 72; (b) Buss, J. A.; Agapie, T., Mechanism of Molybdenum-Mediated Carbon Monoxide Deoxygenation and Coupling: Mono- and Dicarbyne Complexes Precede C–O Bond Cleavage and C–C Bond Formation. *Journal of the American Chemical Society* **2016**, *138* (50), 16466-16477; (c) Horak, K. T.; VanderVelde, D. G.; Agapie, T., Tuning of Metal Complex Electronics and Reactivity by Remote Lewis Acid Binding to π -Coordinated Pyridine Diphosphine Ligands. *Organometallics* **2015**, *34* (19), 4753-4765; (d) Horak, K. T.; Lin, S.; Rittle, J.; Agapie, T., Heterometallic Effects in Trinuclear Complexes Supported by p-Terphenyl Diphosphine Ligands. *Organometallics* **2015**, *34* (18), 4429-4432; (e) Edouard, G. A.; Kelley, P.; Herbert, D. E.; Agapie, T., Aryl Ether Cleavage by Group 9 and 10 Transition Metals: Stoichiometric Studies of Selectivity and Mechanism. *Organometallics* **2015**, *34* (21), 5254-5277; (f) Horak, K. T.; Agapie, T., Dioxide Reduction by a Pd(0)–Hydroquinone Diphosphine Complex. *Journal of the American Chemical Society* **2016**, *138* (10), 3443-3452; (g) Buss, J. A.; Edouard, G. A.; Cheng, C.; Shi, J.; Agapie, T., Molybdenum Catalyzed Ammonia Borane Dehydrogenation: Oxidation State Specific Mechanisms. *Journal of the American Chemical Society* **2014**, *136* (32), 11272-11275; (h) Henthorn, J. T.; Agapie, T., Modulation of Proton-Coupled Electron Transfer through Molybdenum–Quinonoid Interactions. *Inorganic Chemistry* **2016**, *55* (11), 5337-5342; (i) Henthorn, J. T.; Lin, S.; Agapie, T., Combination of Redox-Active Ligand and Lewis Acid for Dioxide Reduction with π -Bound Molybdenum–Quinonoid Complexes. *Journal of the American Chemical Society* **2015**, *137* (4), 1458-1464; (j) Tsui, E. Y.; Agapie, T., Carbon dioxide cleavage by a Ni₂ complex supported by a binucleating bis(N-heterocyclic carbene) framework. *Polyhedron* **2014**, *84*, 103-110; (k) Lin, S.; Herbert, D. E.; Velian, A.; Day, M. W.; Agapie, T., Dipalladium(I) Terphenyl Diphosphine Complexes as Models for Two-Site Adsorption and Activation of Organic Molecules. *Journal of the American Chemical Society* **2013**, *135* (42), 15830-15840; (l) Suseno, S.; Horak, K. T.; Day, M. W.; Agapie, T., Trinuclear Nickel Complexes with Metal–Arene Interactions Supported by Tris- and Bis(phosphinoaryl)benzene Frameworks. *Organometallics* **2013**, *32* (23), 6883-6886; (m) Horak, K. T.; Velian, A.; Day, M. W.; Agapie, T., Arene non-innocence in dinuclear complexes of Fe, Co, and Ni supported by a para-terphenyl diphosphine. *Chemical Communications* **2014**, *50* (34), 4427-4429; (n) Lin, S.; Day, M. W.; Agapie, T., Nickel Hydrides Supported by a Non-Innocent Diphosphine Arene Pincer: Mechanistic Studies of Nickel–Arene H-Migration and Partial Arene Hydrogenation. *Journal of the American Chemical Society* **2011**, *133* (11), 3828-3831; (o) Chao, S. T.; Lara, N. C.; Lin, S.; Day, M. W.; Agapie, T., Reversible Halide□ Modulated Nickel–Nickel Bond Cleavage: Metal–Metal Bonds as Design Elements for Molecular Devices. *Angewandte Chemie International Edition* **2011**, *50* (33), 7529-7532.
6. (a) Halter, D. P.; Heinemann, F. W.; Bachmann, J.; Meyer, K., Uranium-mediated electrocatalytic dihydrogen production from water. *Nature* **2016**, *530*, 317; (b) Bart, S. C.; Heinemann, F. W.; Anthon, C.; Hauser, C.; Meyer, K., A New Tripodal Ligand System with Steric and Electronic Modularity for Uranium Coordination Chemistry. *Inorganic Chemistry* **2009**, *48* (19), 9419-9426; (c) Fieser, M. E.; Palumbo, C. T.; La Pierre, H. S.; Halter, D. P.; Voora, V. K.; Ziller, J. W.; Furche, F.; Meyer, K.; Evans, W. J., Comparisons of lanthanide/actinide +2 ions in a tris(aryloxy)arene coordination environment. *Chemical Science* **2017**, *8* (11), 7424-7433.
7. (a) Nyulászi, L.; Veszprémi, T.; D'S, B. A.; Verkade, J., Photoelectron Spectra and Structures of Proazaphosphatranes. *Inorganic Chemistry* **1996**, *35* (21), 6102-6107; (b) Tang, J. S.; Verkade, J. G., Synthesis and reactivity patterns of new proazaphosphatranes and quasi-azaphosphatranes ZP(MeNCH₂CH₂)₃N. *Journal of the American Chemical Society* **1993**, *115* (5), 1660-1664; (c) Liu, X.-D.; Verkade, J. G., Unusual Phosphoryl Donor Properties of OP(MeNCH₂CH₂)₃N. *Inorganic Chemistry* **1998**, *37* (20), 5189-5197; (d) Laramay, M. A. H.; Verkade, J. G., The "anomalous" basicity of P(NHCH₂CH₂)₃N relative to P(NMeCH₂CH₂)₃N and p(NbCH₂CH₂)₃N: a chemical consequence of orbital charge balance? *Journal of the American Chemical Society* **1990**, *112* (25), 9421-9422; (e) Liu, X.; Bai, Y.; Verkade, J. G., Synthesis and structural features of new sterically hindered azaphosphatrane systems: ZP(RNCH₂CH₂)₃N. *Journal of Organometallic Chemistry* **1999**, *582* (1), 16-24; (f) Kárpáti, T.; Veszprémi, T.; Thirupathi, N.; Liu, X.; Wang, Z.; Ellern, A.; Nyulászi, L.; Verkade, J. G., Synthesis and Photoelectron Spectroscopic Studies of N(CH₂CH₂NMe)₃P(E) (E = O, S, NH, CH₂). *Journal of the American Chemical Society* **2006**, *128* (5), 1500-1512.
8. (a) Tang, J.; Mohan, T.; Verkade, J. G., Selective and Efficient Syntheses of Perhydro-1,3,5-triazine-2,4,6-triones and Carbodiimides from Isocyanates Using ZP(MeNCH₂CH₂)₃N Catalysts. *The Journal of Organic Chemistry* **1994**, *59* (17), 4931-4938; (b) Liu, X.; Verkade, J. G., Free and Polymer-Bound Tricyclic Azaphosphatranes HP(RNCH₂CH₂)₃N⁺: Procatalysts in Dehydrohalogenations and Debrominations with NaH. *The Journal of Organic Chemistry* **1999**, *64* (13), 4840-4843; (c) Arumugam, S.; McLeod, D.; Verkade, J. G., Use of the Nonionic Superbase

- P(MeNCH₂CH₂)₃N in the Selective Monoalkylation of Active-Methylene Compounds. *The Journal of Organic Chemistry* **1998**, *63* (11), 3677-3679; (d) Kisanga, P.; McLeod, D.; D'S, B.; Verkade, J., P(RNCH₂CH₂)₃N-Catalyzed Synthesis of β-Hydroxy Nitriles. *The Journal of Organic Chemistry* **1999**, *64* (9), 3090-3094; (e) Ilankumaran, P.; Verkade, J. G., P(RNCH₂CH₂)₃N: Efficient Catalysts for Transesterifications, Acylations, and Deacylations. *The Journal of Organic Chemistry* **1999**, *64* (9), 3086-3089.
9. (a) Lensink, C.; Xi, S. K.; Daniels, L. M.; Verkade, J. G., The unusually robust phosphorus-hydrogen bond in the novel cation [cyclic] HP(NMeCH₂CH₂)₃N⁺. *Journal of the American Chemical Society* **1989**, *111* (9), 3478-3479; (b) Kisanga, P. B.; Verkade, J. G.; Schwesinger, R., pK_a Measurements of P(RNCH₂CH₂)₃N. *The Journal of Organic Chemistry* **2000**, *65* (17), 5431-5432; (c) D'Sa, B.; Kisanga, P.; McLeod, D.; Verkade, J., P(RNCH₂CH₂)₃N: Superbasic and Catalytic Dages. *Phosphorus, Sulfur, and Silicon and the Related Elements* **1997**, *124* (1), 223-232; (d) Wroblewski, A. E.; Pinkas, J.; Verkade, J. G., Strongly basic proazaphosphatranes: P(EtNCH₂CH₂)₃N and P(iso-PrNCH₂CH₂)₃N. *Main Group Chem.* **1995**, *1* (1), 69-79.
10. Green, M. L. H.; Parkin, G., The classification and representation of main group element compounds that feature three-center four-electron interactions. *Dalton Transactions* **2016**, *45* (47), 18784-18795.
11. Kisanga, P.; McLeod, D.; Liu, X.; Yu, Z.; Ilankumaran, P.; Wang, Z.; McLaughlin, P. A.; Verkade, J. G., New Chemistry of ZP(RNCH₂CH₂)₃N Systems. *Phosphorus, Sulfur, and Silicon and the Related Elements* **1999**, *144* (1), 101-104.
12. (a) Xi, S. K.; Schmidt, H.; Lensink, C.; Kim, S.; Wintergrass, D.; Daniels, L. M.; Jacobson, R. A.; Verkade, J. G., Bridgehead-bridgehead communication in untransannulated phosphatranes ZP(ECH₂CH₂)₃N systems. *Inorganic Chemistry* **1990**, *29* (12), 2214-2220; (b) Windus, T. L.; Schmidt, M. W.; Gordon, M. S., Theoretical Investigation of Azaphosphatranes Bases. *Journal of the American Chemical Society* **1994**, *116* (25), 11449-11455; (c) Tang, J. S.; Laramay, M. A. H.; Verkade, J. G., Chemical and structural implications of bond formation between the bridgehead atoms in Z-P(MeNCH₂CH₂)₃N systems. *Phosphorus, Sulfur Silicon Relat. Elem.* **1993**, *75* (1-4), 205-8; (d) Laramay, M. A. H.; Verkade, J. G., Unusually Lewis basic Proazaphosphatranes. *Zeitschrift für anorganische und allgemeine Chemie* **1991**, *605* (1), 163-174; (e) Chatelet, B.; Gornitzka, H.; Dufaud, V.; Jeanneau, E.; Dutasta, J.-P.; Martinez, A., Superbases in Confined Space: Control of the Basicity and Reactivity of the Proton Transfer. *Journal of the American Chemical Society* **2013**, *135* (49), 18659-18664; (f) Liu, X.; Ilankumaran, P.; Guzei, I. A.; Verkade, J. G., P[(S,S,S)-PhHMeCNCH₂CH₂]₃N: A New Chiral 31P and ¹H NMR Spectroscopic Reagent for the Direct Determination of ee Values of Chiral Azides. *The Journal of Organic Chemistry* **2000**, *65* (3), 701-706; (g) Raytchev, P. D.; Martinez, A.; Gornitzka, H.; Dutasta, J.-P., Encaging the Verkade's Superbases: Thermodynamic and Kinetic Consequences. *Journal of the American Chemical Society* **2011**, *133* (7), 2157-2159; (h) Galasso, V., Theoretical Study of the Structure and Bonding in Phosphatranes Molecules. *The Journal of Physical Chemistry A* **2004**, *108* (20), 4497-4504.
13. Tang, J. S.; Laramay, M. A. H.; Young, V.; Ringrose, S.; Jacobson, R. A.; Verkade, J. G., Stepwise transannular bond formation between the bridgehead atoms in Z-P(MeNCH₂CH₂)₃N systems. *Journal of the American Chemical Society* **1992**, *114* (8), 3129-3131.
14. (a) Su, W.; Urgaonkar, S.; Verkade, J. G., *Org. Lett.* **2004**, *6*, 1421-1424; (b) Urgaonkar, S.; Nagarajan, M.; Verkade, J. G., *Tetrahedron Lett.* **2002**, *43*, 8921-8924; (c) You, J.; Verkade, J. G., *J. Org. Chem.* **2003**, *68*, 8003-8007.
15. (a) Nandakumar, M. V.; Verkade, J. G., One-Pot Sequential N and C Arylations: An Efficient Methodology for the Synthesis of trans 4-N,N-Diaryl Aminostilbenes. *Angewandte Chemie International Edition* **2005**, *44* (20), 3115-3118; (b) Venkat Reddy, C. R.; Urgaonkar, S.; Verkade, J. G., *Org. Lett.* **2005**, *7*, 4427-4430; (c) Urgaonkar, S.; Nagarajan, M.; Verkade, J. G., *J. Org. Chem.* **2003**, *68*, 452-459.
16. Aneetha, H.; Wu, W.; Verkade, J. G., Stereo- and Regioselective Pt(DVDS)/P(iBuNCH₂CH₂)₃N-Catalyzed Hydrosilylation of Terminal Alkynes. *Organometallics* **2005**, *24* (11), 2590-2596.
17. (a) Thammavongsy, Z.; Kha, I. M.; Ziller, J. W.; Yang, J. Y., Electronic and steric Tolman parameters for proazaphosphatranes, the superbase core of the tri(pyridylmethyl)azaphosphatranes (TPAP) ligand. *Dalton Transactions* **2016**, *45* (24), 9853-9859; (b) Thammavongsy, Z.; Khosrowabadi Kotyk, J. F.; Tsay, C.; Yang, J. Y., Flexibility is Key: Synthesis of a Tripyridylamine (TPA) Congener with a Phosphorus Apical Donor and Coordination to Cobalt(II). *Inorganic Chemistry* **2015**, *54* (23), 11505-11510; (c) Chatelet, B.; Nava, P.; Clavier, H.; Martinez, A., Synthesis of Gold(I) Complexes Bearing Verkade's Superbases. *European Journal of Inorganic Chemistry* **2017**, *2017* (37), 4311-4316.
18. Yang, L.; Powell, D. R.; Houser, R. P., Structural variation in copper(i) complexes with pyridylmethylamide ligands: structural analysis with a new four-coordinate geometry index, [small tau]4. *Dalton Transactions* **2007**, *9* (9), 955-964.
19. Frisch, M. J.; Trucks, G. W.; Schlegel, H. B.; Scuseria, G. E.; Robb, M. A.; Cheeseman, J. R.; Scalmani, G.; Barone, V.; Petersson, G. A.; Nakatsuji, H.; Li, X.; Caricato, M.; Marenich, A. V.; Bloino, J.; Janesko, B. G.; Gomperts, R.; Mennucci, B.; Hratchian, H. P.; Ortiz, J. V.; Izmaylov, A. F.; Sonnenberg, J. L.; Williams, Ding, F.; Lipparini, F.; Egidi, F.; Goings, J.; Peng, B.; Petrone, A.; Henderson, T.; Ranasinghe, D.; Zakrzewski, V. G.; Gao, J.; Rega, N.; Zheng, G.; Liang, W.; Hada, M.; Ehara, M.; Toyota, K.; Fukuda, R.; Hasegawa, J.; Ishida, M.; Nakajima, T.; Honda, Y.; Kitao, O.; Nakai, H.; Vreven, T.; Throssell, K.; Montgomery Jr., J. A.; Peralta, J. E.; Ogliaro, F.; Bearpark, M. J.; Heyd, J. J.; Brothers, E. N.; Kudin, K. N.; Staroverov, V. N.; Keith, T. A.; Kobayashi, R.; Normand, J.; Raghavachari, K.; Rendell, A. P.; Burant, J. C.; Iyengar, S. S.; Tomasi, J.; Cossi, M.; Millam, J. M.; Klene, M.; Adamo, C.; Cammi, R.; Ochterski, J. W.; Martin, R. L.; Morokuma, K.; Farkas, O.; Foresman, J. B.; Fox, D. J. *Gaussian 16 Rev. B.01*, Wallingford, CT, 2016.
20. Zhao, Y.; Truhlar, D. G., The M06 suite of density functionals for main group thermochemistry, thermochemical kinetics, noncovalent interactions, excited states, and transition elements: two new functionals and systematic testing of four M06-class functionals and 12 other functionals. *Theoretical Chemistry Accounts* **2008**, *120* (1), 215-241.
21. Verkade, J. G., P(RNCH₂CH₂)₃N: Very Strong Non-Ionic Bases Useful in Organic Synthesis. In *New Aspects in Phosphorus Chemistry II*, Majoral, J.-P., Ed. Springer Berlin Heidelberg: Berlin, Heidelberg, 2003; pp 1-44.
22. Aghazadeh Meshgi, M.; Zitz, R.; Walewska, M.; Baumgartner, J.; Marschner, C., Tuning the Si-N Interaction in Metalated Oligosilanylsilatrane. *Organometallics* **2017**, *36* (7), 1365-1371.
23. Brennan, M. R.; Kim, D.; Fout, A. R., A synthetic and mechanistic investigation into the cobalt(i) catalyzed amination of aryl halides. *Chemical Science* **2014**, *5* (12), 4831-4839.
24. Useful Reagents and Ligands. In *Inorganic Syntheses*, John Wiley & Sons, Inc.: 2002; pp 75-121.
25. Harris Robin, K.; Becker Edwin, D.; Cabral de Menezes Sonia, M.; Goodfellow, R.; Granger, P., NMR nomenclature. Nuclear spin properties and conventions for chemical shifts (IUPAC Recommendations 2001). In *Pure and Applied Chemistry*, 2001; Vol. 73, p 1795.

